ELSEVIER

Chemical Engineering Journal 87 (2002) 111–120

Chemical Engineering Journal

www.elsevier.com/locate/cej

Adsorption of lindane from water onto GAC: effect of carbon loading on kinetic behavior

J.L. Sotelo*, G. Ovejero, J.A. Delgado, I. Martínez

Faculty of Chemistry, Department of Chemical Engineering, Universidad Complutense de Madrid, Av. Complutense s/n, 28040 Madrid, Spain

Accepted 17 September 2001

Abstract

Batch kinetic experiments of adsorption of lindane in dilute aqueous solution onto F-400 granular activated carbon (GAC) with different carbon weight and initial concentration were analyzed. Concentration decay of lindane was measured by means of SPME (solid phase micro extraction). A high level of energetic and structural heterogeneity of the F-400 activated carbon was observed by means of TG analysis. An adsorption model including film-, macropore-, and micropore-diffusion based on the branched pore model was fitted to experimental data. The effect of carbon loading on model parameters can be summarized as follows: (i) the effective macropore diffusivity, including pore and surface diffusivity, and the micropore rate coefficient have little dependence on carbon loading, and (ii) the fraction of adsorptive capacity in macropores depends strongly on carbon loading, which is attributed to the difference in adsorptive affinity in macro- and micropores.

Keywords: Lindane; Activated carbon; Adsorption kinetics; SPME

1. Introduction

Organic pesticides have been present in raw water supplies since about 1940. They are toxic and hazardous to various target organisms, including humans. The chemical and biological stability of many pesticides, together with their hydrophobic behavior, has made adsorption onto activated carbon a feasible and effective treatment for their removal. Lindane (γ-isomer of hexachlorocyclohexane) is one example of these compounds [1]. This pesticide has a broad range of application [2], and it is included in the environmental protection agency's (EPA) list of organic priority pollutants [3]. This contaminant has been detected in surface water sources at residual levels up to 0.15 $\mu g\,l^{-1}$ [4]. There is some information in the literature concerning the adsorption of lindane on activated carbon [1,5]. These studies show that activated carbon can be used to reduce the concentration of this pesticide down to the potable level, but no information is given about the parameters needed to describe the dynamics of the system. Kouras et al. [4] studied the aqueous adsorption kinetics of lindane onto powdered activated carbon, using an empirical model to describe the experimental results. Although this kind of models are widely used to design adsorption systems, models with a theoretical basis have some advantages in this respect because a wider range of conditions, as well as a larger number of variables, can be considered.

The design of adsorption systems requires to obtain the solute concentration decay curves for the sorbate/sorbent system as the starting point, as well as the adsorption capacity of the sorbent as a function of sorbate concentration (adsorption isotherm). The description of adsorption kinetics involves the comparison of the experimental concentration decay curves with those predicted with a model, which can have an empirical or theoretical basis, in order to estimate the kinetic parameters. Several models can be proposed depending on the mechanism of transport assumed inside the particle, which can be diffusion in the liquid-filled pores, diffusion in the adsorbed phase (surface diffusion) and both mechanisms in parallel. The literature is rich with research work on the description of adsorption systems with theoretical models. The pore diffusion model was used by Liapis and Rippin [6] to describe literature data of the adsorption of alcohols on activated carbon and by Garcia et al. [7] for the adsorption of phenolic mixtures on a polymeric adsorbent. The model that has probably received more attention is the homogeneous solid diffusion model (HSDM), which is based on the assumption that the concentration in the internal liquid-phase is negligible and surface diffusion dominates. This model has been used by Crittenden and Weber [8,9], Al-Duri and McKay [10] and McKay [11]. Chatzopoulos et al. [12] used

* Corresponding author. Tel.: +34-91-3944117; fax: +34-91-3944114.
E-mail address: chejls@eucmax.sim.ucm.es (J.L. Sotelo).

1385-8947/02/$ – see front matter
PII: S1385-8947(01)00223-6

Nomenclature

c	concentration in the pores ($mg\,l^{-1}$)
C	liquid-phase concentration ($mg\,l^{-1}$)
d	diameter (cm)
D	diffusivity in macropores ($cm^2\,s^{-1}$)
E	characteristic energy of the D–R equation ($J\,mol^{-1}$)
f	fraction of adsorptive capacity in the macropore region
$\langle f \rangle$	average fraction of adsorptive capacity in the macropore region
H	Henry's law constant
k_b	micropore rate coefficient (s^{-1})
k_L	external mass transfer coefficient ($cm\,s^{-1}$)
K_F	Freundlich constant
n	adsorbed-phase concentration (mg in macro- or micropore region/g)
n_F	Freundlich exponent
N	impeller speed (s^{-1}); number of experimental points
p_i	empirical parameter i
q	adsorbed phase concentration (mg (g of macro- or micropore region, or including both regions)$^{-1}$)
r	radial variable (cm)
R	particle radius (cm); gas constant ($J\,mol^{-1}\,K^{-1}$)
RMS	parameter defined in Eq. (19)
t	time (s)
T	temperature (K)
V	liquid volume (l)
W	mass of carbon (g)

Greek letters

α	particle porosity
ρ	particle density ($g\,cm^{-3}$)
τ	tortuosity

Subscripts and superscripts

b	branch or micropore
e	equilibrium in all the adsorbent particle
m	macropore
p	pore; particle
s	surface; saturation
T	including macro- and micropores
0	initial value
$*$	effective value

this model taking into account that surface diffusivity depends on concentration. Models considering both mechanisms in parallel have been used by Neretnieks [13], Fritz et al. [14], Costa et al. [15] and Calleja et al. [16]. Advanced models take into account the structural heterogeneity of activated carbon by assuming a bidisperse structure [17].

The aim of this paper is to study the adsorption kinetics of lindane onto granular activated carbon (GAC) in a batch system. A wide concentration interval was considered both in equilibrium and kinetic experiments, reaching the maximum level permitted by European legislation ($0.1\,\mu g\,l^{-1}$). A model assuming a bidisperse structure (macro- and micropores), each region having different adsorption isotherm, was used to describe the system, and the effect of carbon loading on kinetic behavior was studied by changing both the initial concentration of sorbate and the sorbent weight.

2. Experimental

2.1. Materials and methods

Lindane (99%) was supplied by Sigma. Alachor (2-chloro-2′,6′diethyl-*N*-methoxymethylacetanilide) (99.4%) was supplied by Chem Service. Solutions were prepared with distilled water passed through a Milli-Q water purifier (Millipore Corporation). The sorbent was a commercial GAC, Filtrasorb 400, supplied by Chemviron Carbon. The sieve fraction between 0.84 and 1 mm was selected. The activated carbon was stored at 110 °C, boiled in water during 20 min, and cooled by adding water prior to use. The physical properties of the carbon were determined by N_2 porosimetry (Asap 2000, Micromeritics) and Hg porosimetry (Pascal 240, Fisons), and the results are shown in Table 1.

Experimental solutions were prepared by adding weighed amounts of lindane to water in a Pyrex flask, leaving the solution under heating and stirring with reflux overnight, and letting the solution cool down to room temperature. Solutions of $10\,mg\,l^{-1}$ prepared with this method were transparent, and no crystallization of lindane was observed in several months.

Equilibrium experiments were performed in 0.2 l Pyrex flasks using the bottle-point technique, including a blank. Weighed amounts of sorbent were added to each bottle containing a solution of lindane. The bottles were immediately closed and agitated in a constant temperature bath until equilibrium was reached. The initial concentration was the same for all the bottles ($10\,mg\,l^{-1}$). Contact time in equilibrium

Table 1
Physical properties of F-400 activated carbon

BET surface area ($m^2\,g^{-1}$)	1070
Skeletal density ($g\,cm^{-3}$)	2.400
Pore volume ($cm^3\,g^{-1}$)	
Micropores ($d_p < 20$ Å)	0.475
Mesopores ($20 < d_p < 500$ Å)	0.052
Macropores ($d_p > 500$ Å)	0.355
Total	0.882
Particle density[a] ($g\,cm^{-3}$)	0.770
Average particle size (cm)	0.092

[a] Density (Hg).

experiments was 1 month enough to reach equilibrium conditions. No change of concentration was observed in the blank experiment. The adsorbed concentration at equilibrium, q_e, was obtained from the mass balance equation with the equilibrium liquid concentration, C_e,

$$q_e = \frac{V}{W}(C_0 - C_e) \quad (1)$$

where V is the solution volume, W the sorbent weight, and C_0 the initial liquid concentration.

Kinetic experiments were conducted in a 5 l Pyrex spherical tank, provided with a four-bladed, flat stainless steel impeller, and four baffles. A Heidolph Type RZR1 variable speed motor was used to drive the impeller. A constant temperature bath containing the tank was also used. Samples of 10 ml approx. were taken at several times and centrifuged to prevent fine carbon particles caused by attrition from affecting the analysis, which was observed in preliminary experiments. Nevertheless, the samples were always transparent, indicating that the level of attrition was very low. No variation in size or shape of the initial carbon granules was detectable after being recovered and dried. Since, the total extracted volume was very small compared to the total one, it was considered that the liquid volume remained constant during each experiment. Both equilibrium and kinetic experiments were done at 25 °C.

The carbon sample studied by TG was prepared by immersing 31 mg of carbon into 0.5 l of a lindane solution with an initial concentration of 10 mg l^{-1}. After a month at room temperature, the liquid concentration was 0.018 mg l^{-1}. The carbon loading was estimated with Eq. (1), resulting in 161 mg g^{-1}. The carbon particles were separated and dried at room temperature. A virgin carbon sample boiled in water and dried at room temperature, and a carbon sample loaded with alachlor from an aqueous solution of 10 mg l^{-1} and dried in the same way, were subjected to same analysis for comparison.

2.2. Analytical procedures

Analyses were carried out by means of SPME (solid phase micro extraction) and gas chromatography. A manual SPME holder was used with a 100 μm poly(dimethylsiloxane) fiber assembly (Supelco). Samples with concentration higher than 0.1 mg l^{-1} were diluted by 1/100. Samples were placed in 4 ml vials, each of them containing a magnetic bar. The vials were placed in an SPME sampling stand (Supelco), which was lying on a heat/stir plate. The fiber was immersed into the sample. Extraction time was 5 min at 40 °C with agitation. The fiber was then immediately inserted into the GC injector, and the analysis was performed. The desorption time was 5 min and the desorption temperature was set at 250 °C. A Varian 3400 gas chromatograph fitted with a 15 m × 0.25 mm i.d. 0.25 μm film column packed with SPB-5 (Supelco) and equipped with a ^{63}Ni electron capture detector (ECD) was employed for the analysis. Nitrogen was used as a carrier gas. Temperatures for the injector and the detector were 250 and 200 °C, respectively. A calibration curve of peak areas vs. concentration was used for concentration determination. Each sample was analyzed at least two times, resulting in relative standard deviations of peak areas of about 6%. From the estimation of the proportionality constant between the peak area and the mass of lindane injected (using a lindane solution in *n*-hexane of 10 mg l^{-1}), it was estimated that the fiber/water concentration ratio obtained with the analytical method described above was about 250.

Thermogravimetrical analysis was performed with a Exstar TG/DTA 6200 equipment (Seiko Instruments), with a flow of helium of 100 ml min^{-1} and a heating rate of 10 °C min^{-1}.

3. Model description

A model based on the biporous structure proposed by Peel et al. [17] was used to describe the kinetic behavior of the system lindane–GAC. In this model, the carbon particle is partitioned into two regions: macropores, in which an initial rapid uptake occurs; and micropores, in which restricted diffusion takes place and the remaining capacity to equilibrium is utilized. As micropores branch off macropores, mass transfer proceeds through three different steps coupled in series: (i) mass transfer from fluid phase to particle surface, (ii) diffusion in the macropore region and (iii) diffusion in the micropore region. However, a different approach is proposed to define the fraction of macropore region. In the model of Peel et al. [17], the fraction of macropore region (both in weight and volume) is represented by the parameter f, and the following equations are applicable when equilibrium is reached:

$$f\left(\frac{\text{g of macropore region}}{\text{g of particle}}\right) q_m^e \left(\frac{\text{mg of solute}}{\text{g of macropore region}}\right) + (1-f)\left(\frac{\text{g of micropore region}}{\text{g of particle}}\right) \times q_b^e \left(\frac{\text{mg of solute}}{\text{g of micropore region}}\right) = q_T^e \left(\frac{\text{mg of solute}}{\text{g of particle}}\right) \quad (2)$$

$$q_m^e \left(\frac{\text{mg of solute}}{\text{g of macropore region}}\right) = q_b^e \left(\frac{\text{mg of solute}}{\text{g of micropore region}}\right) = q_T^e \left(\frac{\text{mg of solute}}{\text{g of particle}}\right) \quad (3)$$

For this model, the parameter f is expected to be constant since it is related to the pore volume distribution of the sorbent. In Eq. (3), it is implicitly assumed that the isotherms in macro- and micropores (in the units indicated) are the same

as the total isotherm (measured experimentally). However, this assumption is not realistic, since the energetic distribution is different in macro- and micropores. The true equilibrium condition is the equality of chemical potentials, not the equality of adsorbed concentrations. It is reasonable to propose a less favorable isotherm in macropores. In order to consider this possibility in the model, new variables have been defined with the units (mg in macropore region)/(g of total particle) (n_m) and mg in micropore region g^{-1} of total particle (n_b). Therefore, at equilibrium, the total adsorptive capacity is expressed as the sum of two terms

$$q_T^e(C_e) = n_m^e(C_e) + n_b^e(C_e) \tag{4}$$

The total isotherm, which can be obtained experimentally, results from the sum of the isotherms in macro- and micropores. Accordingly, the total adsorbed-phase concentration in a spherical differential volume with thickness dr at any time is divided in two fractions; n_m, in equilibrium with the corresponding liquid concentration (c_m), and n_b, for which the liquid-phase is considered negligible. The spatial coordinate for the flux in macropores is the radial direction, whereas the one for micropores is perpendicular to it. Therefore, the flux in the radial direction only occurs through macropores. The mass balance in macropores is given by

$$\alpha_m \frac{\partial c_m}{\partial t} + \rho \frac{\partial n_m}{\partial t} = \frac{1}{r^2}\frac{\partial}{\partial r}\left(r^2 D_p^* \frac{\partial c_m}{\partial r}\right) - \rho R_b \tag{5}$$

where α_m is the macropore fraction (cm^3 macropore/cm^3 particle), D_p^* the effective macropore diffusivity (referred to the total particle cross-sectional area) and R_b the rate of transfer from the macropore network to the micropores or branched pores (mg/(g s)). The mass balance in micropores is expressed as

$$\frac{\partial n_b}{\partial t} = R_b \tag{6}$$

The isotherm in macropores can be described as a fraction of the total experimental isotherm

$$n_m^e = f q_m^e(c_m) \tag{7}$$

where the parameter f now represents the fraction of adsorptive capacity in macropores ($f \leq 1$). It is important to note that this parameter may depend on concentration. The adsorptive affinity is normally lower in macropores, so it may be expected that the curvature of the isotherm in this region is lower than the one of the total isotherm, leading to a concentration-dependent f. For example, if the isotherm in macropores is linear, and the total isotherm is favorable, f increases with concentration ($f(c) = n_m^e(c)/q_T^e(c)$). A constant average value of f was considered as a fitting parameter of the model for each kinetic run ($\langle f \rangle$), which may depend on the concentration interval of the experiment.

The following equation can be proposed for R_b, assuming a linear driving force between macro- and micropores

$$R_b = k_b'((1 - \langle f \rangle) q_T(c_m) - n_b) \tag{8}$$

which is based on the fact that the adsorbed concentration at the micropore mouth is in equilibrium with $c_m(n_b = (1-\langle f \rangle) q_T)$, so that the proposed linear driving force is valid to quantify the deviation from equilibrium in micropores for a given c_m. The parameter k_b' represents a micropore rate coefficient. There exists a simple relationship between this parameter and the micropore rate coefficient (k_b, Eq. (9)) proposed by Peel et al. [17]

$$(1 - f)\frac{\partial q_b}{\partial t} = k_b(q_T(c_m) - q_b) \tag{9}$$

Rewriting Eq. (8)

$$R_b = \frac{\partial n_b}{\partial t} = k_b'(1 - \langle f \rangle)\left(q_T(c_m) - \frac{n_b}{1 - \langle f \rangle}\right) \tag{10}$$

Introducing a change of variable ($q_b = n_b/(1 - \langle f \rangle)$),

$$(1 - \langle f \rangle)\frac{\partial q_b}{\partial t} = k_b'(1 - \langle f \rangle)(q_T(c_m) - q_b) \tag{11}$$

So it is deduced that $k_b = k_b'(1 - \langle f \rangle)$. For the sake of comparison with literature results, k_b was considered as the fitting parameter representing the micropore rate coefficient. On this basis, the macropore mass balance can be written as follows:

$$\frac{\partial c_m}{\partial t} = \frac{(1/r^2)(\partial/\partial r)(r^2 D_p^*(\partial c_m/\partial r)) - \rho k_b(q_T(c_m) - (n_b/(1 - \langle f \rangle)))}{\alpha_m + \rho \langle f \rangle (dq_T/dc_m)} \tag{12}$$

The micropore mass balance is

$$\frac{\partial n_b}{\partial t} = k_b\left(q_T(c_m) - \frac{n_b}{1 - \langle f \rangle}\right) \tag{13}$$

The differential external mass balance is given by

$$V\frac{dC}{dt} = -\frac{3W}{\rho R}\left(D_p^* \frac{\partial c_m}{\partial r}\right)_{r=R} \tag{14}$$

C being the solute concentration in the tank, V the volume of the liquid-phase, W the mass of sorbent and R the particle radius.

The initial and boundary conditions are

$$\begin{aligned} &t = 0, \quad C = C_0, \qquad t = 0, \quad 0 < r < R, \\ &c_m = 0, \quad n_m = 0, \qquad t > 0, \quad r = 0, \\ &\frac{\partial c_m}{\partial r} = 0, \quad \frac{\partial n_m}{\partial r} = 0 \end{aligned} \tag{15}$$

C_0 being the initial value of solute concentration. Coupling between the liquid and solid phases is achieved by equating the fluxes at the solid–liquid interface:

$$k_L(C - c_{r=R}) = \left(D_p^* \frac{\partial c_m}{\partial r}\right)_{r=R} \tag{16}$$

where k_L is the external mass-transfer coefficient.

The effective macropore diffusivity is

$$D_p^* = \alpha_m \frac{D_m}{\tau} + \rho D_s \frac{dn_m}{dc_m} \quad (17)$$

where D_m is the free molecular diffusivity of the sorbate in the solvent, τ the tortuosity, D_s the surface diffusivity, and dn_m/dc_m the slope of the adsorption isotherm in macropores. In this work, it was assumed that the effective pore diffusivity was constant, which is equivalent to assume that the product $D_s(dn_m/dc_m)$ is constant. The free molecular diffusivity of lindane was estimated from a literature correlation, resulting in $5.65 \times 10^{-6}\,cm^2\,s^{-1}$ [18]. The value of α_m was set to 0.31 according to the pore volume distribution (including macro- and mesoporosity, Table 1). The tortuosity was set to 4, an intermediate value within the typical range of this parameter (2–6 [19]). The assumption of constant effective pore diffusion in the adsorption onto activated carbon, in systems where surface diffusion is the controlling step, has been validated in the literature by several authors [14,16,20]. It is valid for systems with linear isotherm or with energetic heterogeneity where the decrease of the slope of the adsorption isotherm compensates for the increase of surface diffusivity when the concentration inside the sorbent increases, which usually applies in the adsorption of organic solutes onto activated carbon. Nevertheless, many adsorption studies in the literature are based on the application of a kinetic model with constant surface diffusivity rather than constant pore diffusivity, probably because this model is more intuitive when surface diffusion dominates the internal transport. Neretnieks [13] showed that there exists an approximate relationship between the effective pore diffusivity and the effective surface diffusivity (assumed to be constant) in a batch system, which has been adapted to the biporous model

$$D_p^* = \alpha_m \frac{D_m}{\tau} + \rho \langle D_s \rangle \frac{n_m(C_0)}{C_0} = \alpha_m \frac{D_m}{\tau} + \rho \langle D_s \rangle \frac{f(q_0) q_0}{C_0} \quad (18)$$

where $\langle D_s \rangle$ is the effective surface diffusivity, and q_0 the total adsorbed concentration in equilibrium with C_0. The parameter $\langle D_s \rangle$ represents an average value of macropore surface diffusivity for a kinetic run in a batch system, which depends on the equilibrium adsorbed concentration in each run [21]. An expression similar to Eq. (18) has been proposed elsewhere to relate the effective pore and surface diffusivities in a GAC column [22].

4. Numerical methods

The best parameter values for all the fitting procedures performed in this work were calculated as those that minimize the root mean square (RMS) of the normalized residuals, defined in Eq. (19)

$$\mathrm{RMS} = \left[\frac{1}{N} \sum_{i=1}^{i=N} \left(\frac{y_{exp,i} - y_{cal,i}}{y_{exp,i}} \right)^2 \right]^{12} \times 100 \quad (19)$$

where N is the number of experimental points and y the dependent variable. This objective function was used because the range of y_{exp} (concentration) was of several orders of magnitude, all the values of y_{exp} having the same importance in Eq. (19). A FORTRAN subroutine available in the literature based on the Nelder and Mead optimization procedure was employed for this purpose [23]. A first estimation of the adjustable parameters was made by comparing the calculated curves with the experimental results visually, in order to start the minimization procedure. The 95% confidence limits of the parameter values were estimated on linear hypothesis [24].

The method of orthogonal collocation [25] was used to discretize the set of PDEs resulting from the model in the radial coordinate. A FORTRAN subroutine based on the Runge–Kutta–Fehlberg method [26] was employed to integrate the ordinary differential equations resulting from each model analyzed. The concentration at the particle surface for a given time is calculated introducing the external concentration and the concentration at the internal collocation points in Eq. (16), since the gradient at the particle surface is a linear combination of the concentrations at the collocation points, including the concentration at the macropore mouth. This method includes an adaptive step size procedure. Six collocation points proved to be sufficient to observe no change in the calculated evolution of solute concentration.

For the two-resistance model considering the dependence on concentration of surface diffusivity explicitly, the PDECOL package was used [27], which is based on the method of orthogonal collocation in finite elements. The radial coordinate was subdivided in 50 subintervals, with two collocation points in each subinterval, which was enough to observe no change in the calculated evolution of solute concentration. For this model, the mass balance in the pore was written as follows:

$$\frac{\partial c}{\partial t} = \frac{(1/r^2)(\partial/\partial r)(r^2 D_p^* (\partial c/\partial r))}{\alpha + \rho(dq_T/dc)} = \frac{F\nabla^2 c + (dF/dc)(\partial c/\partial r)^2}{\alpha + \rho(dq_T/dc)} \quad (20)$$

where $F = (D_m\alpha/\tau) + \rho D_s(c)(dq/dc)$, this variable replacing the effective pore diffusivity in the boundary condition at the particle surface (Eq. (16)).

5. Results and discussion

5.1. Adsorption equilibrium

Fig. 1 presents equilibrium data for lindane in aqueous solution onto F-400 activated carbon at 25 °C. The

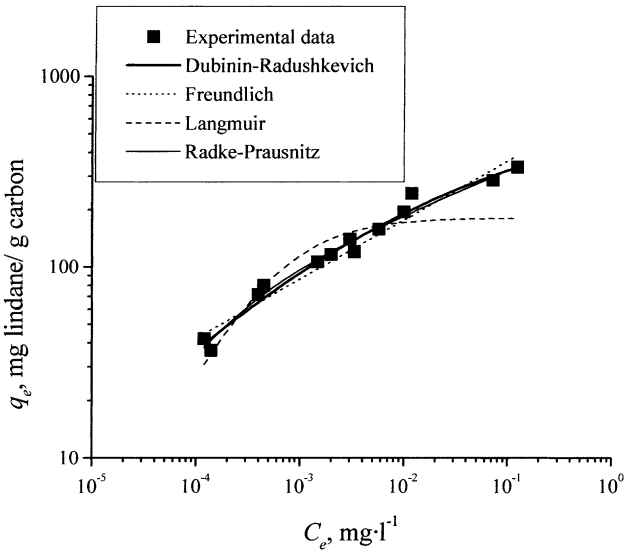

Fig. 1. Equilibrium isotherm for aqueous lindane adsorption on F-400 GAC at 25 °C.

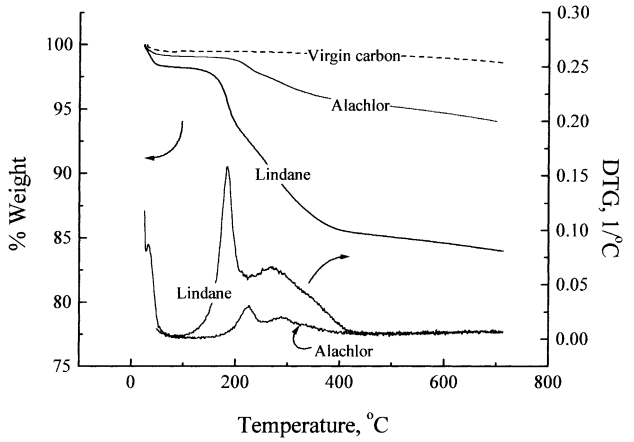

Fig. 2. TG and DTG curves of F-400 GAC loaded with lindane and alachlor, compared to the curves corresponding to the fresh adsorbent.

experimental points were fitted to several well-known equations for adsorption isotherms. Results are presented in Table 2. The Langmuir isotherm gave the poorest fit, deviating considerably at high liquid concentrations, which can be attributed to the energetic heterogeneity of the activated carbon surface. The Freundlich isotherm yielded a better fit, but this equation cannot account for the slight curvature showed by the experimental isotherm on double logarithmic scale in the interval of concentrations studied. The best fit among the two-parameters isotherms was given by the Dubinin–Radushkevich equation, which also yielded optimum values of the parameters with an acceptable level of significance. In order to improve the fitting quality, a three parameter isotherm, the Radke–Prausnitz equation was tested. The improvement of the fit provided by this equation does not compensate for the loss of significance of the new parameters. Therefore, it was discarded and the Dubinin–Radushkevich equation was selected for further use. The value of the parameter E (17 kJ mol^{-1}) in this equation represents an average value of the energy released during the adsorption process. Considering that the upper limit for physical adsorption is about 80 kJ mol^{-1} [3], it is deduced that the adsorption of lindane onto activated carbon has a physical nature. According to this, the thermal desorption of this compound should be relatively easy. In order to study this point, samples of clean carbon boiled in water and carbon loaded with lindane were subjected to thermogravimetric analysis. Results are shown in Fig. 2. From the DTG curve, it was estimated that lindane desorption starts at 100 °C and finishes at 440 °C. Two steps are distinguished in this process, the first from 100 to 230 °C, where the weight percentage changes from 98.23 to 92.55%, and the second from 230 to 440 °C, where the variation is from 98.23 to 85.34%. Thus, the carbon loading estimated from the TG analysis is $(0.9823 - 0.8534)/0.8534 \times 1000 = 151\,\mathrm{mg\,g^{-1}}$, which is similar to that estimated from the mass balance (161 mg g^{-1}). This result agrees with the hypothesis of physical adsorption, since it indicates that little residue remains after desorption. If irreversible adsorption occurs, the thermal treatment generally leads to a significant amount of residue on the carbon [28].

The two steps in the desorption process indicate that there is a change of mechanism in the desorption process, which

Table 2
Parameter and RMS values of the isotherm equations tested

Isotherm model	Parameters values	RMS (%)
Langmuir: $q_e = \frac{q_s b C_e}{1 + bC_e}$	$q_s = 181 \pm 45\,\mathrm{mg\,g^{-1}}$[a], $b = 1705 \pm 1065\,\mathrm{l\,mg^{-1}}$	23.3
Dubinin–Radushkevich[b]:	$q_s = 487 \pm 72\,\mathrm{mg\,g^{-1}}$, $E = 17.7 \pm 0.8\,\mathrm{kJ\,mol^{-1}}$	9.6
$q_e = q_s \exp\left[-\left(\frac{RT}{E}\ln\left(\frac{c_s}{C_e}\right)\right)^2\right]$		9.6
Freundlich: $q_e = K_F C_e^{n_F}$	$K_F = 741 \pm 193\,\mathrm{mg\,g^{-1}(l\,mg^{-1})^{n_F}}$, $n_F = 0.311 \pm 0.04$	14.1
Radke–Prausnitz: $q_e = \left(\frac{1}{AC_e} + \frac{1}{BC_e^d}\right)^{-1}$	$A = (6.98 \pm 4.3) \times 10^5\,\mathrm{mg\,g^{-1}\,l\,mg^{-1}}$, $B = 550 \pm 156\,\mathrm{mg\,g^{-1}\,(l\,mg^{-1})^d}$, $d = 0.230 \pm 0.06$	9.4

[a] 95% confidence limits.
[b] c_s: solubility of lindane in water at 25 °C (10 mg l^{-1}) [2].

could be attributed to the beginning of lindane decomposition at 200 °C. However, this hypothesis was discarded on the grounds of the well-defined boiling point of lindane (323.4 °C [29]). Furthermore, the formation of gaseous components due to decomposition should lead to an increase in weight loss rate with respect to the initial one due to vaporization [28], which does not occur in this case.

This result can derive from the existence of two zones with different adsorption energy for lindane. The first peak in the DTG curve can be attributed to the lindane adsorbed in macropores and the second one to that adsorbed in micropores. The fraction of lindane desorbed in the first step (about 44%) is similar to the fraction of macro- and mesopores deduced from the pore size distribution (46.1%, Table 1), which is in good agreement with this hypothesis. Nevertheless, this similarity must be considered only qualitatively, since not all the pores are accessible to lindane, and the adsorption mechanism in large pores differs significantly from the volumetric filling occurring in micropores. In order to confirm this hypothesis, the same analysis was performed with a carbon sample loaded with alachlor, other chlorinated pesticide (boiling point, 355 °C, supplied by Chem Service), the results being shown in Fig. 2. It is observed that the desorption of this compound follows the same pattern, the desorption occurring at higher temperatures because of its higher boiling point. This result agrees with the hypothesis that the two steps in the desorption process stem from the structural heterogeneity of the adsorbent.

5.2. Adsorption kinetics

A set of kinetic experiments were performed changing the weight of sorbent and the initial liquid concentration. Table 3 shows the conditions of each experiment; concentration decay curves are shown in Fig. 4 (varying carbon weight) and Fig. 5 (varying initial concentration). A change in the slope of the kinetic curve before reaching the equilibrium concentration was observed in all the experiments, which indicates that there is a change in the controlling step of the adsorption process. In preliminary tests, it was observed that two-resistance models were not able to reproduce the experimental data, including a model where the

Table 3
Data of aqueous lindane-activated carbon kinetic runs

Run number[a]	W (g)	C_0 (mg l^{-1})
1	1	10
2	1	10
3	1	0.83
4	1	3.33
5	0.3	10
6	0.5	10
7	4	10
8	8	10

[a] All the experiments have been done at 25 °C, $N = 400$ rpm and with a liquid volume of 3 l.

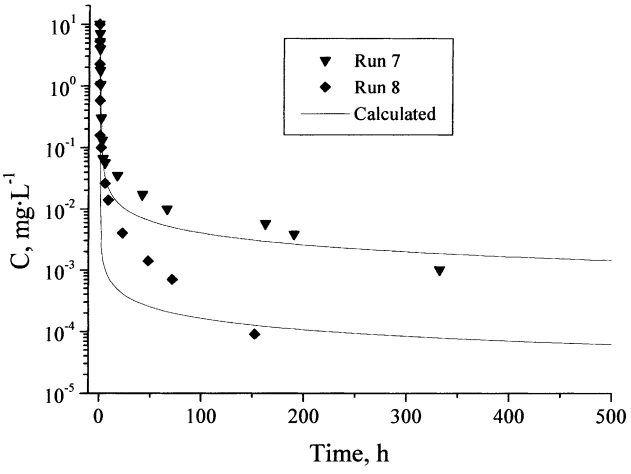

Fig. 3. Comparison of theoretical and experimental curves for the two-resistance model with concentration-dependent surface diffusivity for runs 7 and 8 (Table 3).

dependence of surface diffusivity on concentration was considered explicitly. The equation proposed by Seidel and Carl [30] was used to describe this dependence, taking into account the equilibrium relationship $q(c)$

$$D_s = D_{s0}\left(\frac{c}{c_s}\right)^a \tag{21}$$

where D_{s0} is the surface diffusivity at saturation and a the ratio between the activation energy of surface diffusion and the adsorption energy. The poorest fitting results, which are shown in Fig. 3, were obtained with runs 7 and 8, leading to the following values of the adjustable parameters; run 7, $k_L = 5.4 \times 10^{-3}$ cm s^{-1}, $D_{s0} = 1.6 \times 10^{-9}$ cm^2 s^{-1}, $a = 0.80$, RMS = 38%; run 8, $k_L = 5.5 \times 10^{-3}$ cm s^{-1}, $D_{s0} = 6.8 \times 10^{-9}$ cm^2 s^{-1}, $a = 0.65$, RMS = 59%.

The data from each of the experiments were regressed using the bidisperse model described before, the adjustable parameters being k_L, D_p^*, $\langle f \rangle$ and k_b. A comparison between the calculated and experimental concentration decay curves is shown in Figs. 4 and 5. Best values of adjustable parameters are shown in Table 4. The equilibrium concentration in the adsorbed phase, q_e, for each experiment is included. This variable has been selected as a measure of the carbon loading corresponding to each set of parameters [21]. The results in Figs. 4 and 5 show that the model agree well with the experimental data in the whole range of the adsorption period for all the kinetic runs, verifying the adequacy of the model to the system studied.

5.3. Significance of the external mass transfer coefficient

The calculation of the external mass transfer coefficient by non-linear regression can result in unrealistic values for this parameter, which has been previously observed by some authors [31,32]. From a qualitative point of view, the results in Table 4 show that k_L changes little and randomly, which

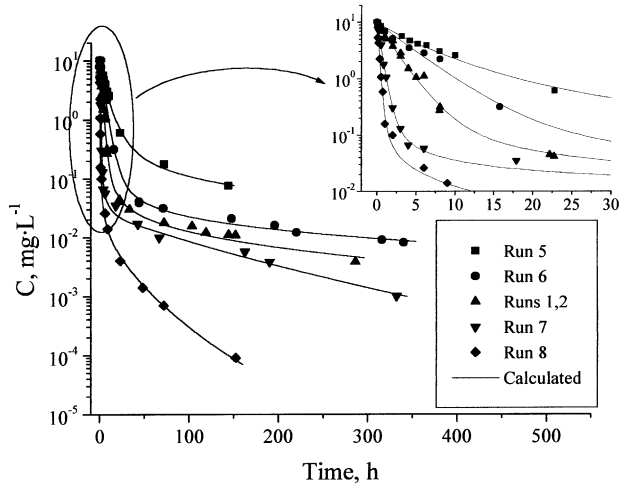

Fig. 4. Effect of the weight of adsorbent on the rate of lindane adsorption on F-400 activated carbon.

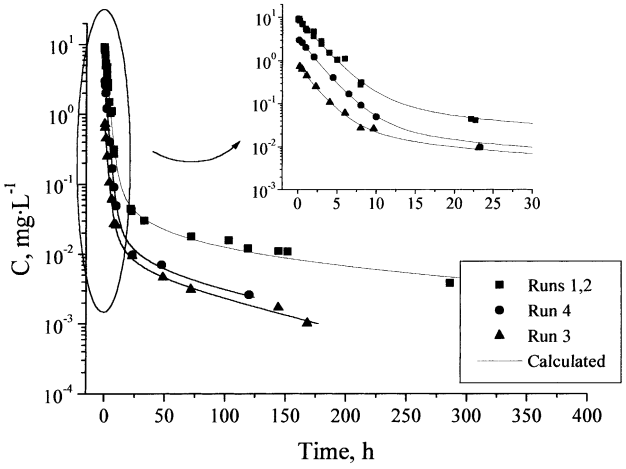

Fig. 5. Effect of the initial concentration on the rate of lindane adsorption on F-400 activated carbon.

is a first indication that the estimated values have physical meaning. The significance of these values has been tested by comparing them to those obtained with several hydrodynamic correlations from literature. Three of these relations have been considered in this study. All of them have the form

$$Sh = 2 + p_1 \left(\frac{\varepsilon d_p^4}{r^3} \right)^{p_2} Sc^{p_3} \quad (22)$$

where the parameters have the following meaning: *Sh*, Sherwood number ($k_L d_p/D_f$); *Sc*, Schmidt number (ν/D_f); ε, power input per unit fluid mass, ($N_{po}N^3T^5/V$); ν, kinematic viscosity of water ($10^{-2}\,cm^2\,s^{-1}$); d_p, particle diameter (Table 1); D_f, free lindane–water diffusivity (estimated) ($5.65 \times 10^{-6}\,cm^2\,s^{-1}$) [18]; N_{po}, power number, 6 [19]; *N*, impeller speed ($6.66\,s^{-1}$); *T*, impeller diameter (5 cm); *V*, liquid volume ($3 \times 10^{-3}\,m^3$). The values of the parameters p_1, p_2 and p_3 for the correlations used in this work and the values of k_L estimated are shown in Table 5. The predicted and experimental values are of the same order of magnitude, so the values of k_L can be considered as significant. The deviation between predicted and estimated values can be ascribed to several reasons: (i) there is an error of 20–30% in the estimation of free liquid diffusivity of the solute with literature correlations [20] and (ii) surface roughness of activated carbon may affect the external mass transfer coefficient [10].

Table 5
Values of the external transfer coefficient estimated with literature correlations

Reference	p_1	p_2	p_3	k_L ($10^{-3}\,cm\,s^{-1}$)
[31]	1.30	0.170	0.25	4.13 (−35%)[a]
[33]	0.64	0.197	0.33	5.03 (−21%)
[19]	0.74	0.175	0.33	4.61 (−27%)

[a] Error with respect to the average value in Table 4.

5.4. Effect of the carbon loading on the internal transport parameters

From the results in Table 4, it is observed that the effect of carbon loading on D_p^* has little significance, this parameter being of the order of $2 \times 10^{-4}\,cm^2\,s^{-1}$. This value is much higher than the effective macropore diffusivity for all the experiments considering diffusion in the liquid-phase only (first term in Eq. (17)). Therefore, the surface diffusion mechanism is dominant for the system lindane-activated

Table 4
Fitting results of the biporous model

Run	q_e ($mg\,g^{-1}$)	k_L ($10^{-3}\,cm\,s^{-1}$)	D_p^* ($10^{-4}\,cm^2\,s^{-1}$)[1]	$\langle f \rangle$	k_b ($10^{-8}\,s^{-1}$)	RMS (%)
5	100	7.4 ± 0.7	1.75 ± 0.3	0.31 ± 0.05	5.8 ± 4.0	8.0
6	60	5.5 ± 0.8	4.50 ± 0.4	0.28 ± 0.04	4.4 ± 3.0	14.0
1, 2	30	5.7 ± 0.8	2.50 ± 0.4	0.18 ± 0.02	4.3 ± 0.5	14.0
4	10	5.7 ± 0.9	4.80 ± 1.7	0.064 ± 0.02	4.6 ± 1.0	5.0
7	7.5	6.5 ± 0.5	2.50 ± 0.5	0.034 ± 0.004	2.4 ± 0.3	12.5
8	3.75	7.0 ± 1.0	3.25 ± 0.5	0.021 ± 0.001	7.2 ± 0.7	18.6
3	2.5	6.6 ± 1.0	3.1 ± 0.6	0.014 ± 0.001	1.5 ± 0.3	8.4

carbon. The average value of the effective macropore diffusivity is similar to those of other solutes adsorbed on activated carbon, for which surface diffusion is also dominant; Calleja et al. [16] obtained values of D_p^* ranging from 0.5 to $5 \times 10^{-4}\,cm^2\,s^{-1}$ for *p*-nitrophenol, and Van Lier [20] obtained values ranging from 0.2 to $4 \times 10^{-4}\,cm^2\,s^{-1}$ for nitrobenzene. Eq. (18) was used for estimating the effective surface diffusivity of lindane on activated carbon for $C_0 = 10\,mg\,l^{-1}$, resulting in $2 \times 10^{-8}\,cm^2\,s^{-1}$, which is of the order of the surface diffusivities of other aqueous organic compounds in activated carbon (*o*-chlorophenol, dichlorophenol, benzoic acid [21]).

Similarly, the effect of carbon loading on k_b is not very strong. This result agrees with that observed by other authors [17,34]. Although the estimation of this parameter is difficult, since long adsorption periods are needed for this parameter to be adequately measured, the linear approach for the micropore transport seems to be adequate for describing the adsorptive behavior of this system in the adsorption period considered. The order of this parameter for lindane in F-400 activated carbon ($10^{-8}\,s^{-1}$) is quite lower than the one of phenol in the same adsorbent ($10^{-6}\,s^{-1}$ [17]), which can be attributed to the higher size of lindane (290 vs. $90\,g\,mol^{-1}$), resulting in a lower diffusivity in micropores.

The dependence of $\langle f \rangle$ on carbon loading is plotted in Fig. 6. It is observed that this dependence is significant for this parameter, $\langle f \rangle$ being quite low at low carbon loadings and tending to an upper limit when q_e increases. This variation must be taken into account to describe the experimental results accurately at low carbon loadings, since the model is very sensitive to the parameter $\langle f \rangle$. This result can be ascribed to the difference in adsorptive affinities in the macro- and micropore regions. At low carbon loadings, the isotherm in micropores is more favorable than the one in macropores, so that the fraction of adsorptive capacity in micropores is increasingly higher as q_e decreases. The effect of q_e on $\langle f \rangle$ can be described with an empirical equation of the form

$$\langle f \rangle = p_4 \left(1 - \frac{1}{1 + \exp((q_T - p_5)/p_6)} \right) \quad (23)$$

Eq. (23) was fitted to the estimated values of $\langle f \rangle$ in Table 4, resulting in the following optimum values of the adjustable parameters: $p_4 = 0.304$, $p_5 = 26.8$, $p_6 = 10.1\,mg\,g^{-1}$, RMS = 35%. Although, Eq. (23) has a empirical nature, it is adequate to consider the theoretical limits of the parameter $\langle f \rangle$. At very low carbon loadings, $\langle f \rangle$ must tend to a constant value, related to the Henry's law constants in macro- and micropores. If $n_m = H_m c$ and $n_b = H_b c$ are the Henry's law isotherms in macro- and micropores respectively, $\langle f \rangle$ must tend to $H_m/(H_m + H_b)$. It is worthwhile mentioning that the assumption of different Henry's law constants in macro- and micropores has already been proposed elsewhere [35]. Therefore, the low value of this parameter observed for lindane at low carbon loadings can be ascribed to a much higher Henry's law constant in micropores. At high carbon loadings, $\langle f \rangle$ must also tend to a finite value, given by the saturation capacities in macro- and micropores. Assuming that the whole pore volume of the particle is filled with solute at saturation, $\langle f \rangle$ must tend to the ratio between macroporosity and total porosity (0.46, Table 1). The upper limit of $\langle f \rangle$ estimated from the kinetic experiments is 0.31, which is lower than this value. This difference may indicate that the macropores are not completely filled in the concentration range studied.

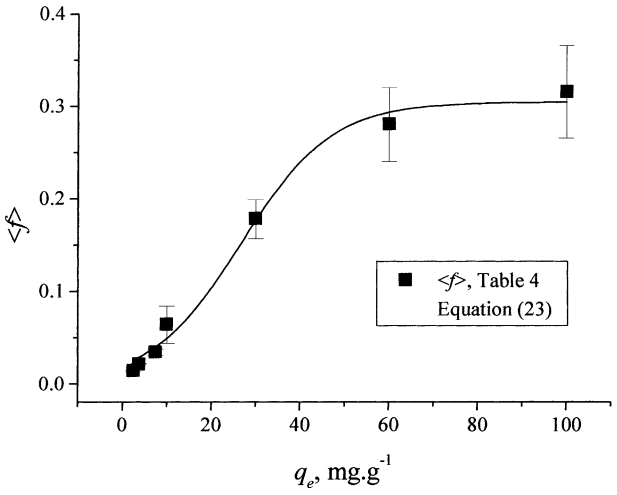

Fig. 6. Effect of the carbon loading on the parameter $\langle f \rangle$.

6. Conclusions

Kinetic and equilibrium data were obtained for the adsorption of aqueous lindane onto GAC for long time periods in a batch system. The best fit to equilibrium data among several well-known two-parameters isotherms was given by the Dubinin–Radushkevich equation. By means of TG analysis, a high level of energetic and structural heterogeneity of the sorbent was observed. These results agree with the energetic heterogeneity inferred from the adsorption equilibrium data.

An adsorption model including film-, macropore-, and micropore-diffusion based on the branched pore theory described the kinetic data satisfactorily. The significance of external mass transfer coefficient was confirmed by comparison of the estimated value by non-linear regression with the one obtained from several literature correlations.

Surface diffusion is the dominant mechanism in the internal transport. The effective macropore diffusivity and the micropore rate coefficient show little dependence on carbon loading. The linear approach for the micropore transport appears quite adequate for describing the adsorptive behavior of this system in the adsorption period considered. The average fraction of adsorptive capacity in macropores depends on carbon loading, which is attributed to the difference in adsorptive affinity in macro- and micropores. This effect

can be described with an empirical expression taking into account the physical limits of this parameter.

Acknowledgements

We gratefully acknowledge financial support from *Comunidad Autónoma de Madrid* (Project 07M/0350/1997).

References

[1] R.A. Hyde, Removal of trace organics from water-1-adsorption of haloforms and chlorinated pesticides by granular activated carbon, Technical Report TR 136, Water Research Centre, 1980.
[2] K.A. Hassal, The Biochemistry and Uses of Pesticides, Structure, Metabolism, Mode of Action and Uses in Crop Protection, 2nd Edition, VCH, Weinheim, 1990.
[3] S.D. Faust, O.M. Aly, Adsorption Processes for Water Treatment, Butterworths, Boston, 1987.
[4] A. Kouras, A. Zouboulis, C. Samara, T. Kouimtzis, Removal of pesticides from aqueous solutions by combined physicochemical processes—the behaviour of lindane, Environ. Pollut. 103 (1998) 193–202.
[5] N.P. Thacker, M.V. Vaidya, M. Sipani, A. Kalra, Removal technology for pesticide contaminants in potable water, J. Environ. Sci. Hlth. B 32 (1997) 483–496.
[6] A.I. Liapis, D.W.T. Rippin, The simulation of binary adsorption in activated carbon columns using estimates of diffusional resistance within the carbon particles derived from batch experiments, Chem. Eng. Sci. 33 (1978) 593–600.
[7] A. Garcia, L. Ferreira, A. Leitao, A. Rodrigues, Binary adsorption of phenol and *m*-cresol mixtures onto a polymeric adsorbents, Adsorption 5 (1999) 359–368.
[8] J.C. Crittenden, W.J. Weber Jr., Predictive model for design of fixed-bed adsorbers: parameter estimation and model development, J. Environ. Eng. Div. (Am. Soc. Civ. Eng.) 104 (1978) 185-197.
[9] J.C. Crittenden, W.J. Weber Jr., Predictive model for design of fixed-bed adsorbers: single-component model verification, J. Environ. Eng. Div. (Am. Soc. Civ. Eng.) 104 (1978) 433–443.
[10] B. Al-Duri, G. McKay, Prediction of binary system for kinetics of batch adsorption using basic dyes onto activated carbon, Chem. Eng. Sci. 46 (1991) 193–204.
[11] G. McKay, Application of surface diffusion model to the adsorption of dyes on bagasse pith, Adsorption 4 (1998) 361–372.
[12] D. Chatzopoulos, A. Varma, R.L. Irvine, Activated carbon adsorption and desorption of toluene in the aqueous phase, AIChE J. 39 (1993) 2027–2041.
[13] I. Neretnieks, Analysis of some adsorption experiments with activated carbon, Chem. Eng. Sci. 31 (1976) 1029–1035.
[14] W. Fritz, W. Merk, E.U. Schlunder, Competitive adsorption of two dissolved organics onto activated carbon-II-adsorption kinetics in batch reactors, Chem. Eng. Sci. 36 (1981) 731–741.
[15] E. Costa, G. Calleja, L. Marijuan, Adsorption of phenol and *p*-nitrophenol on activated carbon: determination of effective diffusion coefficients, Adsorp. Sci. Technol. 4 (1987) 59–77.
[16] G. Calleja, J. Serna, J. Rodríguez, Kinetics of adsorption of phenolic compounds from wastewater onto activated carbon, Carbon 31 (1993) 691–697.
[17] R.G. Peel, A. Benedek, C.M. Crowe, A branched pore kinetic model for activated carbon adsorption, AIChE J. 27 (1981) 26–32.
[18] W.J. Lyman, W.F. Reehl, D.H. Rosenblatt, Handbook of Chemical Property Estimation Methods, McGraw-Hill, New York, 1982.
[19] M. Suzuki, Adsorption Engineering, Kodansha/Elsevier, Tokyo/Amsterdam, 1990.
[20] W.C. Van Lier, Mass transfer to activated carbon in aqueous solutions, Ph.D. Thesis, Delft University of Technology, Delft, the Netherlands, 1989.
[21] Y. Sudo, D.M. Misic, M. Suzuki, Concentration dependence of effective surface diffusion coefficients in aqueous phase adsorption on activated carbon, Chem. Eng. Sci. 33 (1978) 1287–1290.
[22] D.W. Hand, J.C. Crittenden, D.R. Hokanson, J.L. Bulloch, Predicting the performance of fixed-bed granular activated carbon adsorbers, Water Sci. Technol. 35 (1997) 235–241.
[23] W.H. Press, S.A. Teukolsky, W.T. Vetterling, B.P. Flannery, Numerical Recipes in FORTRAN, 2nd Edition, Cambridge University Press, New York, 1992.
[24] F.F. Froment, K.B. Bischoff, Chemical Reactor Analysis and Design, 2nd Edition, Wiley, New York, 1991.
[25] B.A. Finlayson, The Method of Weighted Residuals, Variational Principles, Academic Press, New York, 1972.
[26] J.H. Mathews, Numerical Methods for Computer Science, Engineering and Mathematics, Prentice-Hall, Englewood Cliffs, NJ, 1987.
[27] N.K. Madsen, R.F. Sincovec, PDECOL, general collocation software for partial differential equations [D3], ACM Trans. Math. Software 5 (1979) 326–351.
[28] M. Suzuki, D.M. Misic, O. Koyama, K. Kawazoe, Study of thermal regeneration of spent activated carbons: thermogravimetric measurement of various single component organics loaded on activated carbons, Chem. Eng. Sci. 33 (1978) 271–279.
[29] D.R. Lide (Ed.), Handbook of Chemistry and Physics, 73rd Edition, CRC Press, Boca Raton, FL, 1992.
[30] A. Seidel, P.S. Carl, The concentration dependence of surface diffusion for adsorption on energetically heterogeneous adsorbents, Chem. Eng. Sci. 44 (1989) 189–194.
[31] M.S. Kouyoumdjiev, Kinetics of adsorption from liquid phase on activated carbon, Ph.D. Thesis, Eindhoven University of Technology, Eindhoven, the Netherlands, 1989.
[32] U.K. Traegner, M.T. Suidan, Parameter evaluation for carbon adsorption, J. Environ. Eng. 115 (1989) 109–128.
[33] R.D. Letterman, J.E. Quou, R.S. Gemmell, Film transport coefficient in agitated suspensions of activated carbon, J. Water Pollut. Contr. Fed. 46 (1974) 2536–2546.
[34] A. Leitao, A. Rodrigues, Modelling of solid–liquid adsorption: effects of adsorbent heterogeneity, Chem. Eng. J. 51 (1993) 159–166.
[35] E. Ruckenstein, A.S. Vaidyanathan, G.R. Youngquist, Sorption by solids with bidisperse pore structures, Chem. Eng. Sci. 26 (1971) 1305–1318.